Clays and Clay Minerals, Vol. 68, No. 5:465–475, 2020

SURFACE AND STRUCTURAL PROPERTIES OF CLAY MATERIALS BASED ON NATURAL SAPONITE

O. I. Yanushevska[1]*, T. A. Dontsova[1], A. I. Aleksyk[1], N. V. Vlasenko[2], O. Z. Didenko[2], and A. S. Nypadymka[3]

[1]Department of Inorganic Substances, Water Purification and General Chemical Technology, National Technical University of Ukraine, Igor Sikorsky Kyiv Polytechnic Institute, 37 Peremohy Ave., Kyiv 03056, Ukraine
[2]Department of L.V. Pisarzhevskii Institute of Physical Chemistry of the NAS of Ukraine, 31 Nauky Ave., Kyiv 03028, Ukraine
[3]Department of Technical English №2, National Technical University of Ukraine, Igor Sikorsky Kyiv Polytechnic Institute, 37 Peremohy Ave., Kyiv 03056, Ukraine

Abstract—Because they are so widespread, the use of saponites is significant in many industries. The modification of saponite-rich clay minerals is known to improve their existing characteristics and may provide new functional properties. The objective of the present paper was to characterize the effects of adding nanosized graphene-like molybdenum (Mo) and tungsten (W) sulfides on the textural and surface characteristics of composites based on native saponite and saponite pre-modified with nanoscale magnetite. The textural characteristics were investigated by the nitrogen adsorption-desorption method and scanning electron microscopy. The total acidity, Hammett Brönsted centers, and Quasi-Equilibrium Thermo Desorption (QE-TD) Lewis centers were characteristics used to probe the acid-base properties of the modified composites. In all cases, modification proved to have a significant effect on both the surface and textural properties of the clay matrix. Modification of the native saponite by graphene-like Mo and W sulfides resulted in a decrease in the specific surface area, except a slight increase in the surface area of the magnetite-containing saponite was observed. Analysis of the acid-base characteristics of native and magnetite-modified saponite (MMS) indicated the ability of modified MoS_2 and WS_2 additives to alter the acid-base state of the surface. The addition of graphene-like Mo and W sulfides increased the total acidity of native and MMS, with MoS_2 modification being more promising because, in almost all the samples, saponite composite materials increased the number of both Brönsted and Lewis active centers compared with WS_2, which was determined by the corresponding methods. The acid-base characteristics of the saponite-containing samples, which were studied in an aqueous medium by various methods, are in good correlation with each other, and are consistent with the sorption activity of cationic and anionic dyes.

Keywords—Acid-base properties · Acidity · Hammett method · Modification · Nanosized graphene-like MoS_2 and WS_2 · Saponite nanocomposite materials surface characterization

INTRODUCTION

Saponites are widespread clay minerals found in the weathering zone of magnesium-bearing rocks. Known deposits of saponite are located in Denmark (the Faroe Islands), Japan (Wakamatsu mine), the United States (Montana), and other countries (Treiman et al. 2014; Sokol et al. 2019). The largest deposits in Europe are located in Ukraine, in the Khmelnytskyi region (Ulashaniv, Varvariv, and Tashkiv deposits), with reserves of >30 million tons (Vogels et al. 2005).

Saponites are clay minerals $((M^{+}_{x-y}\cdot nH_2O)(Mg_{3-y}R^{3+}_{y})(Si_{4-x}Al_x)O_{10}(OH)_2$, where R indicates trivalent cation substitutions in the octahedral site, y is the number of trivalent substitutions, M is the exchangeable cation in the interlayer (univalent example given here), x represents the number of substitutions for Si by Al in the tetrahedral sites, and n is a variable). Due to a particular spatial structure, saponites, which are magnesium smectites, exhibit significant adsorption and ion-exchange properties (Hover et al. 1999; Shao and Pinnavaia 2010; Tarasevich et al. 2011; Polyakov and Tarasevich 2012; Vogels et al. 2005).

The use of saponite as a sorption material has been developed widely in many fields of the chemical, agrochemical, food, and medical industries (Choy et al. 2007; Szabo´ et al. 2008; Polyakov and Tarasevich 2012; Chanturiya et al. 2017; Petra et al. 2017; Tangaraj et al. 2017; Kumaresan et al. 2019; Nityashree et al. 2020). The low cost and the wide variety of saponite clay minerals with diverse structural characteristics and sorption properties make them convenient for the formation of high-efficiency low-cost sorbents which can be used in water-purification processes, for example. Acid-activated saponite is used in water-purification processes (Petra et al. 2017; Tangaraj et al. 2017; Zhoua et al. 2019) to remove heavy metal and ammonium ions and is characterized by a large specific surface area, which exceeds significantly the specific surface area of saponite-rich raw material (Rodriguez et al. 1994). Additional modification of saponite by TiO_2 and Ag demonstrated photocatalytic and antibacterial properties for water-purification processes (Fatimaha et al. 2019; Sprynskyya et al. 2019).

Saponite-rich raw material is used successfully as a complex mineral admixture for farm-animal feeds, in the detoxification of anthropogenic and radiation-contaminated soils, as an active sorbent for the extraction of radionuclides and heavy-metal salts from human and animal organisms, plants and nutrition products, and as a preserving agent in root-crop storage, etc. (Murray 1999; Samara et al. 2019). The presence of metal ions such as lithium, chromium, molybdenum, germanium, gold, and

* E-mail address of corresponding author: l_rrr@ukr.net
DOI: 10.1007/s42860-020-00088-4

platinum, in micro-quantities in saponite clay, metals which are vital for human biochemical processes, means that saponite-based medicines offer promise in medical contexts (López-Galindo et al. 2007; Carretero and Pozo 2009; Shao and Pinnavaia 2010; Donauerová et al. 2015; Vogels et al. 2005).

Saponite clay from the Tashkiv deposit (Ukraine) was modified with magnetite nanoparticles (the amounts of Fe_3O_4 in the nanocomposites were 2, 4, 7, and 10 wt.%) (Makarchuk et al. 2017a, c). The modification by magnetite resulted in an increase in the specific surface area and in the sorption activity of these composites to various forms of dye. In the present study, the next step was implemented, i.e. the study of the effect of additives such as nanosized graphene-like molybdenum and tungsten sulfides on the surface and textural characteristics of composites based on native saponite and MMS. The layered chalcogenides of transition metal elements (Mo, W) are known to have significant sorption, photocatalytic, and semiconductor properties with a small energy gap width (ΔE (MoS_2) = 1.84 eV, ΔE (WS2) = 1.97 eV) (Hu et al. 2010; Borisenko et al. 2016; Qiao et al. 2016). Such properties of layer graphene-like chalcogenides of Mo and W and the large specific surface area of nanosized MoS_2 particles (Dontsova et al. 2017) make them interesting in terms of the formation of active sorbent surfaces on clay materials.

Previous results and the unique properties of the graphene-like chalcogenides of Mo and W indicate that an investigation of the effects of modification in texture of saponite-rich raw material and magnetite-containing saponite should be interesting for their future use as sorbents and/or catalysts. This investigation involves the study of the solid phase and acid-base characteristics in both aqueous and air environments. The objective of the present study was to identify the effect of modification of native and MMS with graphene-like Mo and W sulfides on the surface (acid-base) and textural characteristics of the composites with the purpose of creating sorption and/or catalytic materials based on them.

MATERIALS AND METHODS

Saponite

The saponite clay used in the present study is from the Tashkiv deposit (Khmelnytsky region, Ukraine), and is a trioctahedral smectite; for the present study the <63 μm particle-size fraction was used. In previous research (Makarchuk et al. 2017a, b), the chemical composition of the saponite was given as (wt.%): Mg (5.34–7.18); Al (4.90–5.76); Si (20.68–22.67); S (0.00–0.18); Ti (2.22–2.98); V (0.15–0.20); Mn (0.87–1.21); Ca (24.57–26.86); Fe (35.94–37.35); Ni (0.05–0.12); Cu (0.11–0.14); Zn (0.09–0.18); Sr (0.05–0.1). Other mineral phases present in the raw material include quartz and calcite.

Reagents

The reagents used to define the acid-base and sorption properties were obtained from: Carlo Erba Reagents (Chaussée du Vexin, France) for fuchsine, bromophenol blue, methyl red, bromothymol blue, phenol red, thymol blue, indigo carmine, methylene blue, and congo red; Mainchem Co., Ltd. (Xiamen, China) for o-nitro aniline; and Merck & Co. (Kenilworth, New Jersey, USA) for μ-dinitrobenzene.

Magnetic fluid and Magnetic Sorbents. Synthesis of magnetic fluid and magnetic sorption of nanomaterials, with a magnetite particle size of up to 10 nm was implemented following the procedure described in detail by Mykhailenko et al. (2015) and Makarchuk et al. (2017b).

Dichalcogenides. Mo and W chalcogenides (MoS_2 and WS_2) (Vasilyeva et al. 2015) were used as modifiers of native saponite and MMS. Graphene-like 2H MS_2 nanoparticles (M = Mo, W) were obtained by chemical-vapor deposition (CVD) at low temperature (650–670 K) in self-oscillating temperature modes (2015).

Modification by Dichalcogenides

Modification of saponite and MMS was conducted in the following order: water paste-like slurries of saponite clay and MMS were prepared using an ultrasonic (40 kHz) bath (UZM-004-1, Medpromplylad Ltd., Ukraine). After the formation of a suspension of saponite or MMS, modifying metal chalcogenides (Mo, W) were added and mixed for 30 min, then dried for 120 min in a drying chamber at 80°C. Six samples were obtained (Table 1).

Characterization of the Samples Obtained

Specific Surface Area of Saponite Composite Materials. The structural adsorption properties of the composite materials were analyzed using a Quantachrome Autosorb Nova 2200e (Boynton Beach, Florida, USA) instrument. The specific surface area and pore-size distribution were calculated using the Brunauer-Emmett-Teller (BET) equation and the Barrett-Joyner-Halenda (BJH) method, respectively (Brunauer et al. 1938; Villarroel-Rocha et al. 2014) (following Method BS 4359-1:1996 (ISO 9277:1995)). The weight of the sample was 0.3 g, the temperature of adsorption of the adsorbate gas (nitrogen) was 77 K, the pressure in the inert gas (helium) supply line was 70 kPa, and the degassing temperature was 400°C.

SEM. Morphological analysis of the composite samples was conducted using a scanning electron microscope (SEM-106I, Selmi Ltd., Ukraine). Precise chemical analysis of the surface was conducted in each case. The SEM-106I has a built-in microanalysis system with a database of recorded standards for all pure elements.

Acid-Base Properties of Sorbent Surface. The pH of the suspensions of all composite samples was determined using a pH-meter (Portlab 102 pH-Meter, Russia). A 1% suspension of each sample was prepared in twice-distilled water and the change in the pH of the resulting suspension was recorded at regular intervals (t, s). From the data obtained, a pH = f(t) dependence diagram was constructed (Fig. 4).

The effect of the distribution of the sorbent surface centers on the acid-base characteristics was studied by means of the

https://doi.org/10.1007/s42860-020-00088-4 Published online by Cambridge University Press

Table 1. Compositions of six saponite-based, modified sorbents (wt.%)

Sample	Magnetite content	MoS_2 content	WS_2 content	Saponite content
Saponite	–	–	–	100
Sap+MoS_2	–	1	–	99
Sap+WS_2	–	–	1	99
MMS	7	–	–	93
MMS+ MoS_2	7	1	–	92
MMS+ WS_2	7	–	1	92

Hammett method in aqueous solutions (Hammett and Deyrup 1932). For the study, the following dyes (Hammett indicators) were selected: o-nitro aniline (pK = −0.29), fuchsine (pK = 2.1), bromophenol blue (pK = 3.9), methyl red (pK = 5.25), bromothymol blue (pK = 6.8), phenol red (pK = 7.6), thymol blue (pK = 8.8), indigo carmine (pK = 12.8), and μ-dinitrobenzene (pK = 16.8). The sample weight was 0.02 g. The number of centers (q, μg/L g) at a given acid strength was calculated by the formula:

$$q = \frac{C_i \cdot V_i}{D_0} \cdot \left(\frac{|D_0 - D_1|}{m_1} \pm \frac{|D_0 - D_2|}{m_2} \right) \quad (1)$$

where C_i and V_i are the concentration and volume (μg L^{-1} and L, respectively) of the indicator; m_1 and m_2 are the mass of sorbent sample while measuring D_1 and D_2 (g); D_0 is the optical density of initial solutions of indicators; D_1 is the optical density of the solutions after the establishment of adsorption equilibrium and

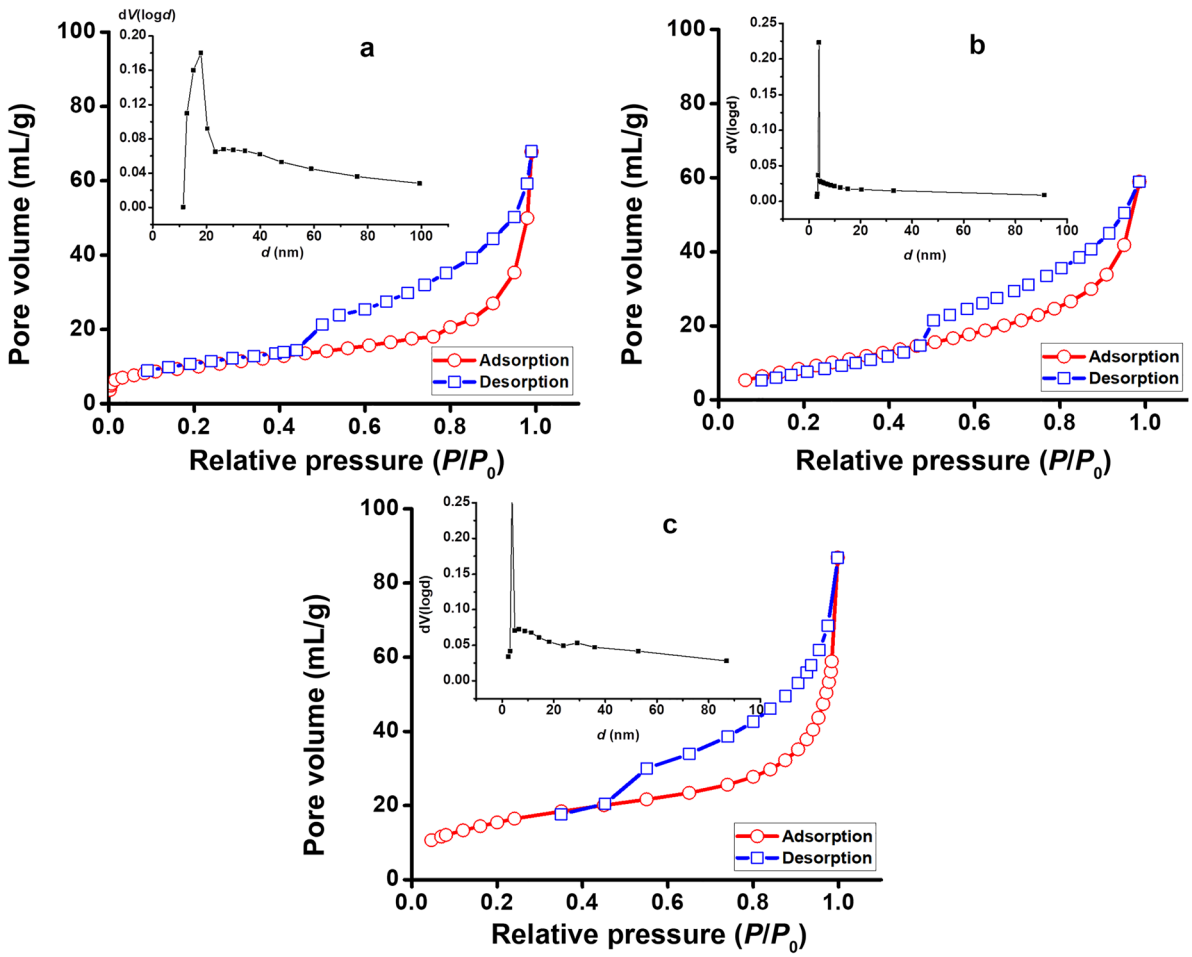

Fig. 1 Nitrogen adsorption-desorption isotherms for **a** saponite, **b** Sap+MoS_2, **c** Sap+WS_2

https://doi.org/10.1007/s42860-020-00088-4 Published online by Cambridge University Press

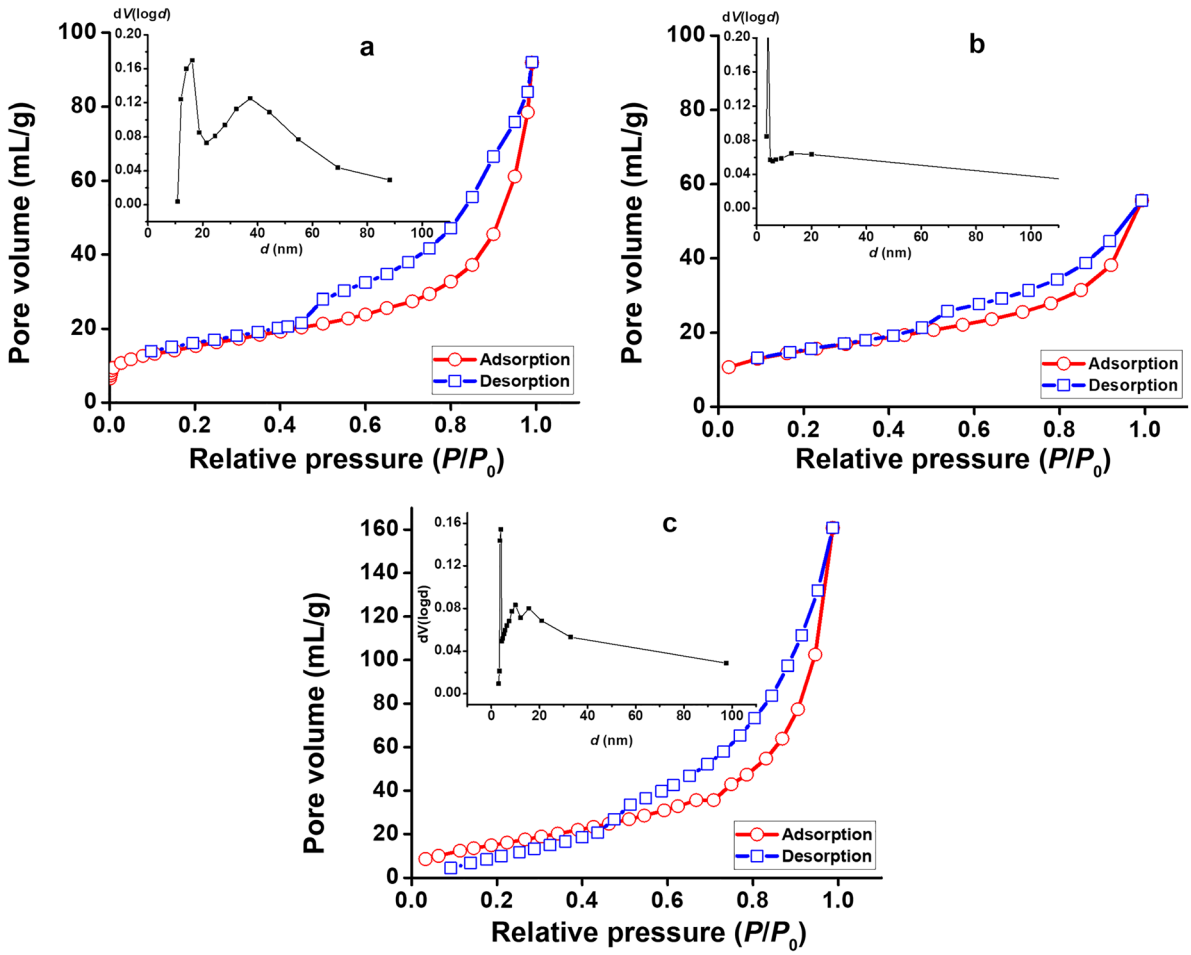

Fig. 2 Nitrogen adsorption-desorption isotherms for **a** MMS, **b** MMS+MoS_2, **c** MMS+WS_2

decantation of the solid phase; D_2 is the optical density, which takes into account the effect of changes in the pH of the medium upon contact of the solution with the sorbent; D_0, D_1, and D_2 were measured simultaneously in parallel experiments. Application of the Hammett method in aqueous solutions was described in detail by Dontsova et al. (2018).

Vacuum Thermogravimetric Method for Determining the Acid-base Characteristics of a Solid Substance. Acid and base properties of the samples were investigated by the Quasi-Equilibrium Thermo Desorption (QE-TD) method. Stepwise thermodesorption of ammonia experiments were conducted at 50–400°C under vacuum (constant pressure of 0.133 Pa was maintained by vacuum pump) using a thermogravimetric apparatus with a quartz spring balance of the McBain type (original handmade equipment). The quasi-equilibrium mode of conducting a thermal desorption experiment suggests that thermal desorption of the probe substance proceeds through the achievement of a sequential series of equilibrium states. The probe substance desorbed during the gradual temperature increase after adsorption onto the test sample. With each temperature-increase increment, the sample was maintained until adsorption equilibrium with a gaseous (CO_2 or NH_3) substance was reached, as measured by the mass "sample + adsorbed substance" (Puziy et al. 2010; Vlasenko et al. 2019a, b). Composite surfaces were degassed to a constant mass by heating the sample in vacuum at 400°C for 15 min (Rodriguez et al. 1994). The number and strength of acid and base centers were evaluated by using ammonia (NH_3) and carbon dioxide (CO_2), respectively, as probes. The temperature was increased stepwise (5°C/min between steps, step size 50°C) with holding at constant temperature until constant weight was achieved at each step for 10–15 min. As a result, the experimental conditions corresponded to the state of adsorption equilibrium of the probe gas at each step.

The amount of probe gas adsorbed per 1 g of solid (Δm) at each temperature was calculated as:

$$\Delta m = \frac{m_{(\text{sample+probe})} - m_{\text{sample}}}{M_{\text{probe}} \times m_{\text{sample}}} \quad (2)$$

where m_{sample} was the mass of the sample before probe adsorption; $m_{(\text{sample+probe})}$ was the mass of a sample with the adsorbed probe gas at a given temperature; M_{probe} is the molecular weight of the probe gas (NH_3 or CO_2).

The differential curves of NH_3/CO_2 sorption were obtained as the differentiatial of the Δm vs T plot using the *Origin* program.

Sorption properties of sorbents. To study the sorption capacity of the composite samples (Saponite, Sap+MoS_2, Sap+WS_2, MMS, MMS+MoS_2, MMS+WS_2), a series of

https://doi.org/10.1007/s42860-020-00088-4 Published online by Cambridge University Press

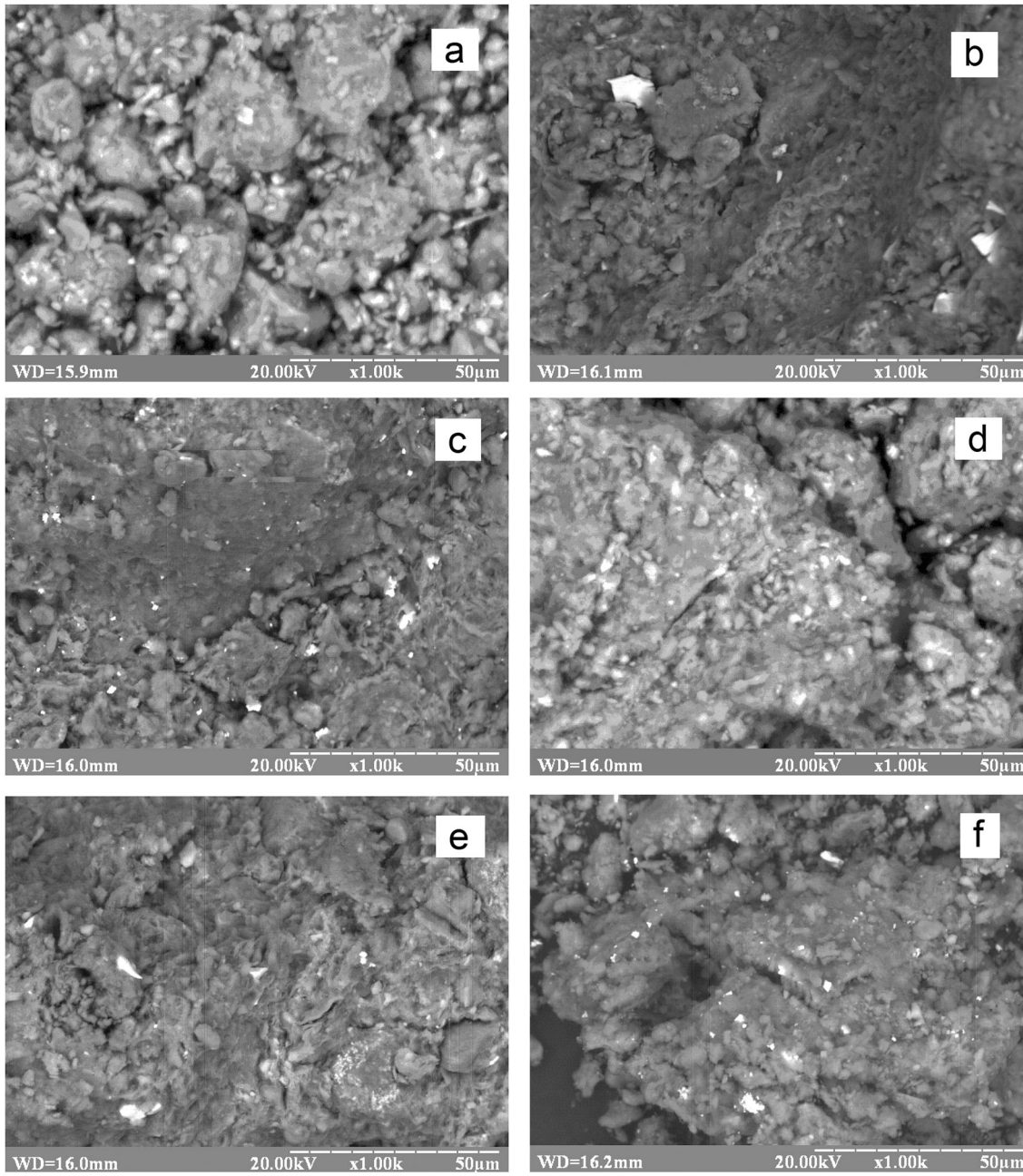

Fig. 3 SEM images of **a** saponite, **b** Sap+MoS_2, **c** Sap+WS_2, **d** MMS, **e** MMS+MoS_2, **f** MMS+WS_2. Scale bars: 50 µm

experiments was carried out in which the adsorption of selected dyes (methylene blue (MB) and congo red (CR)) from their aqueous solutions was measured. To do this, 0.01 g of sorbent was added to the 50 mL solution of the corresponding dye with various concentrations (100 mg/L, 400 mg/L, 600 mg/L, or 1000 mg/L) and mixed in a shaker for 120 min before the establishment of adsorption equilibrium, then the suspension was centrifuged and the separated filtrate was analyzed by spectrophotometry for the presence of residual dye. For the spectrophotometric studies, a 721 UV/Vis Spectrophotometer (Shanghai Metash Instruments Co. Ltd, Shanghai, China) was used. The concentrations of standards used to prepare the calibration curve were: 5, 10, 15, 20, 25, 30, 35, 40, 45, and 50 mg/L. The maximum absorption wavelength for MB was 663 nm and for CR, 490 nm.

The adsorption capacity, q_e (mg g^{-1}), of the sorbents was calculated using Eq. 3:

$$q_e = \frac{(C_0 - C_e)\cdot V}{1000\cdot m_{sorb}} \quad (3)$$

https://doi.org/10.1007/s42860-020-00088-4 Published online by Cambridge University Press

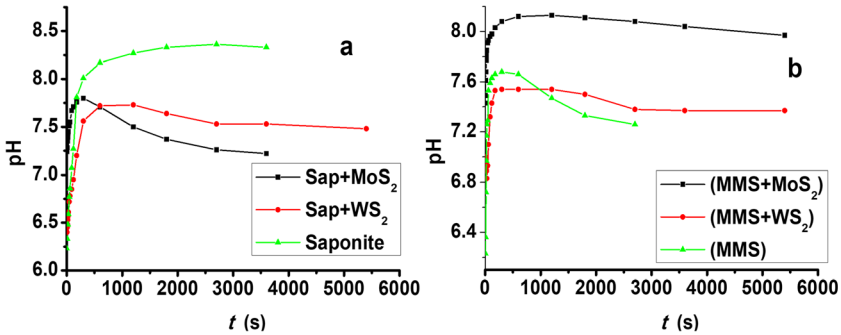

Fig. 4 Time dependence of the total acidity of composites in aqueous suspension

where C_0 and C_e are the initial and residual concentrations of dye (mg g^{-1}), respectively .

RESULTS AND DISCUSSION

Specific Surface Area and Porosity of Saponite Composite Materials

The adsorption-desorption of nitrogen isotherms for all the samples tested (Figs. 1 and 2) revealed that all of the isotherms are type II, and are characteristic of mesoporous materials, and can be described adequately by the BET model. The BET method of surface evaluation of the samples indicated an increase in the specific surface area of magnetite-modified composites compared to the saponite-rich raw material. When saponite was modified with magnetic fluid, the specific surface area of MMS increased from 35 to 53 m^2/g (Figs 1a and 2a). According to the pore distribution curves, both samples exhibited a pronounced mesoporous structure (average pore size of the order of 4 nm), which was due to the porous saponite structure. The pore-size distribution of the MMS sample (Fig. 2a) revealed a maximum of 15 to 18 nm, suggesting that Fe_3O_4 nanoparticles form a secondary mesoporous structure on the saponite surface, i.e. the MMS sample is characterized by bimodality (Dontsova et al. 2018).

Modification of saponite-rich raw material by nanosized graphene-like particles of Mo and W chalcogenides led to the opposite effect compared with magnetite. After the application of MoS_2 and WS_2 (Fig. 1b, c) as modifiers, the specific surface area of the saponite decreased from 35 to 24 and 19 m^2 g^{-1}, respectively, while the average mesopore size remained at 3.96 nm for Sap+MoS_2 and 3.85 nm for Sap+WS_2. The cause of this phenomenon may be the spontaneous conglomeration of chalcogenide nanoparticles due to high natural hydrophobicity in the aquatic environment in the process of sample preparation and blocking of the microporous areas of saponite, resulting in a decrease in specific surface area.

In contrast, when modified by MMS-based chalcogenides (Fig. 2b, c), the specific surface area of the composite increased slightly from 53 m^2 g^{-1} for MMS to 57 and 58 m^2 g^{-1} for MMS+MoS_2 and MMS+WS_2, respectively. This increase in the specific surface area can be explained by the fact that the hydrophobic nanostructured conglomerates of Mo and W sulfides are sorbed onto the secondary mesoporous structure formed by magnetite, which results in the disappearance of the bimodality of the MMS sample. The prevailing pore diameter for these samples was also at the level of 4 nm. In this case, therefore, the incorporation of nanoparticles of chalcogenides of Mo and W into the magnetite-modified saponite contributed to the increase in specific surface area of the composite.

Analyses by SEM (Fig. 3) demonstrated that the morphologies of the saponite and MMS samples are similar, characterized by the existence of separate, distinct particle shapes. The samples of Sap+MoS_2, Sap+WS_2, MMS+MoS_2, and MMS+WS_2 modified by nanosized graphene-like particles of Mo and W chalcogenides differed slightly but were also similar. Compared to the saponite and MMS samples, their surface appeared

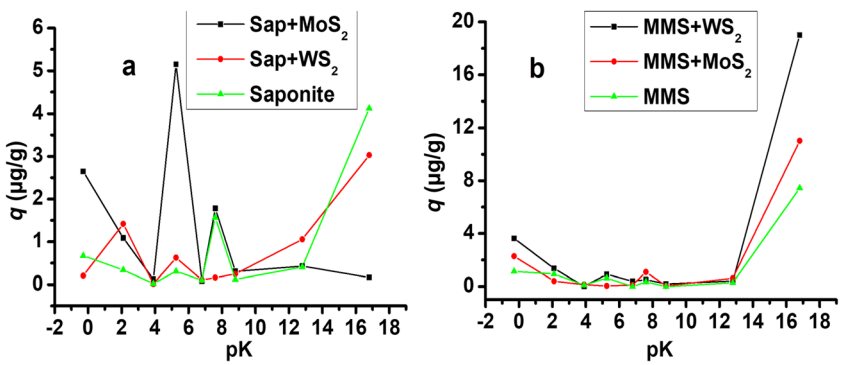

Fig. 5 Distribution of acid and base centers on the surface of composite materials determined by the Hammett method

https://doi.org/10.1007/s42860-020-00088-4 Published online by Cambridge University Press

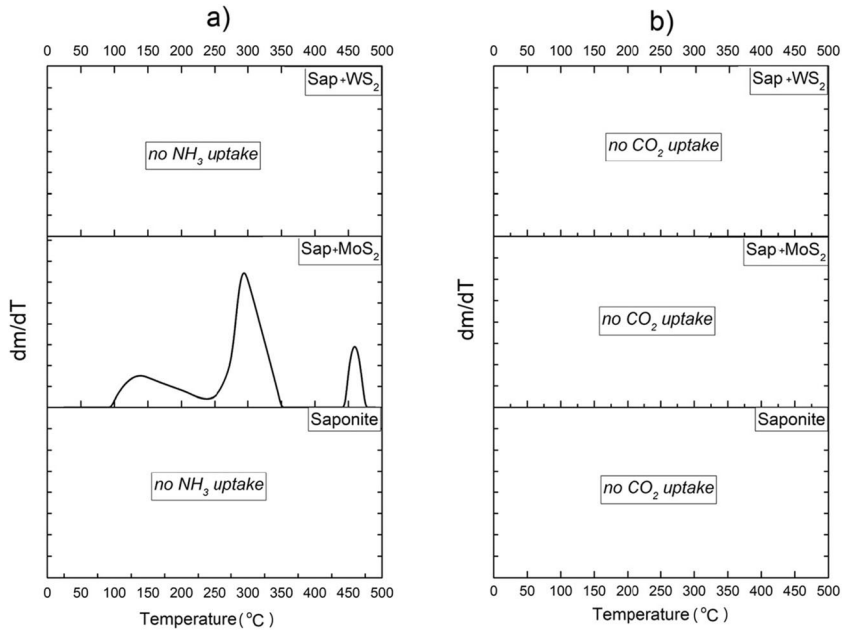

Fig. 6 Differential curves of ammonia desorption for the samples based on saponite

to be covered with a dark layer, indicating deposition of MoS_2 and WS_2 particles on the surface of the saponite and MMS.

As a result of the spot chemical analysis of the Sap+MoS_2, Sap+WS_2, MMS+MoS_2, and MMS+WS_2 surfaces, in addition to the saponite-specific base elements (Si, Al, Fe, Ca, Mg), Mo, W, and S were also detected, which confirmed the deposition of chalcogenides of Mo and W on the surface of the saponite and MMS.

Acid-base Characteristics of the Surface of the Composites

According to modern concepts (Gregg and Sing 1982), the active surface of adsorbents is bifunctional, being a combination of acid and base centers of both the Brönsted and Lewis types. The determination of the nature and concentration of active centers enables prediction, therefore, of the sorption and catalytic abilities of the surface. A fairly accurate method for assessing the acid-base surface properties is the Hammett method, which is implemented in an aqueous medium. A limitation of the method is the possible transformation of the aprotic Lewis centers into Brönsted proton centers in the aqueous medium (Tanabe et al. 1990). This method is, therefore, relevant primarily for characterizing adsorbents and catalysts for processes occurring with the participation of a hydrated solid surface; in particular, water-purification processes. The methods implemented in a gas medium or in a vacuum, when the surface of the material does not undergo changes, are more universal. These methods include quasi-equilibrium thermal desorption. The information obtained with the application of these methods is free from the influence of a solvent and may be useful for predicting the adsorption and catalytic characteristics of materials for a wider range of applications. For this reason, in the current work, study of the active centers of modified composite adsorption was conducted in both aqueous and gas media.

Evaluation of the resulting acidity of the surface in the aqueous medium, performed by measuring the pH of the respective composite suspensions, demonstrated that all the samples had a base characteristic; but, after modification by chalcogenides of Mo and W, a slight increase in the acidity of the modified samples was observed (Fig. 4a,b) indicating a weak hydroxyl-acceptor property of the sample surface (Dai et al. 2017).

This fact correlates well with studies of the distribution of acid-base centers by the Hammett method (Fig. 5a,b). For example, for the MMS sample, the total number of Brönsted acid centers was 1.71 μg g^{-1} in contrast with 0.63 μg g^{-1} for saponite. For Sap+Mo $_2$, Sap+WS_2, MMS+MoS_2, and MMS+WS_2 these values were 6.43, 2.16, 0.7, and 2.68 μg g^{-1}, respectively. The numbers of Brönsted base centers evaluated by the Hammett method for the saponite, MMS, Sap+MoS_2, Sap+WS_2, MMS+MoS_2, and MMS+WS_2 samples were 2.1, 0.63, 2.51, 1.46, 1.75, and 1.11 μg g^{-1}, respectively. These results demonstrated that the number of Brönsted base centers is greatest for saponite and Sap+MoS_2. Modification of saponite material, therefore, led to an increase in the acidic properties of the sorbents. An exception to this was the small but noticeable increase in the basicity of the MMS+MoS_2 sample surface in an aqueous medium, which could probably be explained by the synergistic effect that occurs when both magnetite and molybdenum sulfide are applied.

The work described above demonstrates that additives (magnetite, MoS_2, and WS_2) may enter in ways that cause changes to the textural characteristics and acid-base states of surfaces. The most significant change, namely the increase in

https://doi.org/10.1007/s42860-020-00088-4 Published online by Cambridge University Press

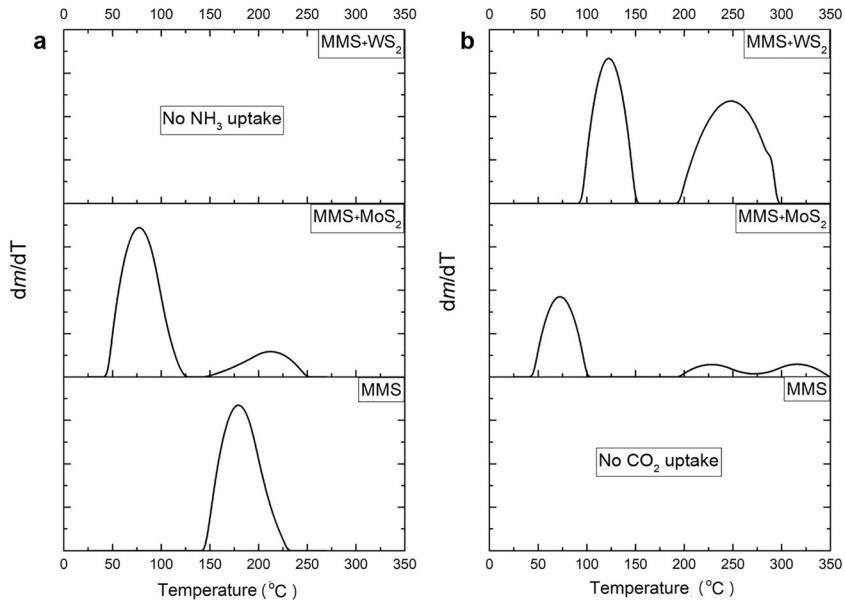

Fig. 7 Differential curves of **a** ammonia and **b** carbon dioxide desorption for the samples based on MMS

the number of active centers, in the surface properties of modified samples of saponite was achieved by using magnetite, and, as already mentioned, by magnetite and nanostructured graphene-like molybdenum sulfide (i.e. their contemporaneous application). More active centers and a larger specific surface area resulted in better sorption properties with respect to pollutants of various natures, as presented by Makarchuk et al. (2017a, b), for the example of magnetite-containing saponite.

Vacuum thermogravimetric studies of the acid-base characteristics of sample surfaces (Figs. 6 and 7) indicated a somewhat different character. According to this technique, acid and base centers were absent from the native saponite. When native saponite was modified with graphene-like WS_2, centers did not appear, but when modified with MoS_2 a small amount (0.28 mmol NH_3 g^{-1}) of the powerful acid centers ($T_{desorption}$ = 475°C) did appear (Table 2).

MMS has some active centers, as shown by the presence of a small number of weak acidic centers (0.08 mmol NH_3 g^{-1}, $T_{desorption}$ = 225°C) on its surfaces. A significant increase in the number and activity of acid centers was observed only after the addition of graphene-like molybdenum sulfide (MMS+MoS_2), characterized by the adsorption of 1.25 mmol NH_3 g^{-1} at 250°C.

The modification of sorbents based on MMS with graphene-like molybdenum sulfide (MMS+MoS_2) generates simultaneously a much smaller number of base centers compared to the number of acid centers, but a much greater force

Table 2. Acid-base characteristics of samples

Sample	Acidity					Basicity				
	C^a, mmol NH_3 g^{-1}				T^*_{des}, NH_3, °C	C^b, mmol CO_2 g^{-1}				T^{**}_{des}, CO_2, °C
	$C^a_{(w)}$	$C^a_{(m)}$	$C^a_{(s)}$	C^a		$C^b_{(w)}$	$C^b_{(m)}$	$C^b_{(s)}$	C^b	
Saponite	No acid capacity					No base capacity				
Sap+MoS_2	0.07	0.18	0.03	0.28	475	No base capacity				
Sap+WS_2	No acid capacity					No base capacity				
MMS	–	0.08	–	0.08	225	No base capacity				
MMS+MoS_2	1.03	0.22	–	1.25	250	0.34	0.07	0.07	0.48	350
MMS+WS_2	No acid capacity					–	0.06	0.08	0.14	300

*Limit strength of acid sites

**Limit strength of base sites

$C^a_{(w)}$, $C^b_{(w)}$: number of weak acid and base centers, respectively; $C^a_{(m)}$, $C^b_{(m)}$: number of medium acid and base centers, respectively; $C^a_{(s)}$, $C^b_{(s)}$: number of strong acid and base centers, respectively; and C^a, C^b: total number of acid and base centers, respectively.

https://doi.org/10.1007/s42860-020-00088-4 Published online by Cambridge University Press

(0.48 mmol CO_2 g^{-1}, $T_{desorption}$ = 350°C) (Fig. 7b). On the other hand, modification of MMS by tungsten sulfide led to the appearance of base centers of average force but only insignificant numbers of them (0.14 mmol CO_2 g^{-1}, $T_{desorption}$ = 300°C). The largest number of acid and base centers occurred, therefore, in the MMS+MoS_2 composite, i.e. saponite modified by nanosized magnetite (7%) and molybdenum sulfide (1%).

The data obtained on the distribution of acid-base centers by vacuum thermogravimetry correlated with the data obtained by the Hammett method, namely, the samples based on saponite-rich raw material were characterized by a smaller total number of acid-base centers than the samples based on MMS. The existing differences in the acidic and basic characteristics of the samples obtained by the different methods (QE-TD method and Hammett method) are explained by the fact that the QE-TD method determines primarily the aprotic Lewis centers, and the Hammett method determines the protonated and hydroxylated Brönsted centers.

These experiments led to the conclusion that the most interesting sorbent was that with magnetite and modified with graphene molybdenum sulfide (MMS+MoS_2), which, compared to other samples, possessed the largest specific surface area (58 m^2 g^{-1}) and the greatest number of acid-base centers, as defined by the Hammett method (6.43 μg g^{-1} of acid centers and 2.51 μg g^{-1} of base centers) and by thermogravimetry (1.25 mmol NH_3 g^{-1}, $T_{desorption}$ = 250°C; 0.48 mmol CO_2 g^{-1}, $T_{desorption}$ = 350°C). This may be related to the synergistic effect between the secondary magnetite structure and the metal chalcogenides.

Analysis of the data above leads to the further conclusion that modification is a powerful tool for changing the surface structure of materials and changing their acid-base characteristics, which may be used to create new sorption and catalytic materials.

Acid-base properties are known to affect sorption and catalytic properties significantly (Tangaraj et al. 2017; Nityashree et al. 2020). In the current paper, testing of the sorption properties of modified and unmodified samples of native and magnetite-containing saponite was motivated by a need to create less expensive saponite-based sorption materials. The sorption capacity of modified and unmodified clay minerals with respect to dyes of various natures relies only on their total acidity (Table 3). Sorbents having base characteristics are more active towards cationic dyes, as evidenced by the increased sorption capacity of twice-modified saponite (MMS+WS_2; 185 μg MB g^{-1} of sorbent) compared to unmodified saponite (103 μg MB g^{-1} of sorbent). A similar situation was observed for the anionic dye, where the sorption capacity of twice-modified MMS+MoS_2 (75 μg CR g^{-1} of sorbent) was greater than for unmodified saponite (39 μg CR g^{-1} of sorbent). An increase in the number of acid or base centers (in this case, the Brönsted centers) after modification led, therefore, to an increase in the sorption activity of both cationic and anionic dyes, which depended also on the specific surface area; the sorption capacity decreased as the specific surface area decreased, and *vice versa*.

Table 3. Sorption capacity of modified and unmodified clay minerals

Sample	Sorption capacity for MB (mg g^{-1})	Sorption capacity for CR (mg g^{-1})
Saponite	103	39
Sap+MoS_2	110	38
Sap+WS_2	90	30
MMS	150	70
MMS+MoS_2	180	75
MMS+WS_2	185	71

CONCLUSIONS

This study of the modification of saponite and MMS by graphene-like MoS_2 and WS_2 revealed the influence of modification on the texture characteristics of composites: the modification of saponite-rich raw material led to a decrease in the specific surface area (from 35 m^2 g^{-1} to 19 m^2 g^{-1}); of MMS, it led to a slight increase (from 53 m^2 g^{-1} to 58 m^2 g^{-1}). The research demonstrated that the acid-base surface state of saponite-rich raw material and MMS changed significantly after their modification by graphene-like MoS_2 and WS_2; the more promising of these is MoS_2. The sorption capacity of the sorbents in relation to cationic and anionic dyes was correlated with the total acidity of the samples. All samples had at least three times greater sorption capacity for cationic than for anionic dyes, which is explained by the general basicity of composite samples. The results showed that targeted modification of relatively inexpensive clay minerals to produce highly efficient sorbents and catalysts with improved surface and texture characteristics is a promising and relevant area in water purification and catalysis. Further studies into catalytic processes are needed, however.

ACKNOWLEDGMENTS

The authors thank Svitlana Nahirniak for her support in conducting this research.

Compliance with Ethical Statements

Conflict of Interest

The authors declare that they have no conflict of interest.

REFERENCES

Borisenko, V. E., Krivosheeva, A. V., & Shaposhnikov, V. L. (2016). Band structure and optical properties of molybdenum and tungsten dichalcogenides. *Bulletin of the Foundation for Fundamental Research, 3*, 41–48 [in Russian].

Brunauer, S., Emmett, P. H., & Teller, E. (1938). Adsorption of gases in multimolecular layers. *Journal of the American Chemical Society, 60*, 309–319.

Carretero, M. I., & Pozo, M. (2009). Clay and non-clay minerals in the pharmaceutical industry: Part I. Excipients and medical applications. *Applied Clay Science, 46*, 73–80.

https://doi.org/10.1007/s42860-020-00088-4 Published online by Cambridge University Press

Chanturiya, V., Minenko, V., Suvorova, O., Pletneva, V., & Makarov, D. (2017). Electrochemical modification of saponite for manufacture of ceramic building materials. *Applied Clay Science, 135*, 199–205.

Choy, J. H., Choi, S. J., Oh, J. M., & Park, M. (2007). Clay minerals and layered double hydroxides for novel biological applications. *Applied Clay Science, 36*, 122–132.

Dai, Q. L., Yan, B., Liang, Y., & Xu, B. Q. (2017). Water effects on the acidic property of typical solid acid catalysts by 3,3-dimethylbut-1-ene isomerization and 2-propanol dehydration reactions. *Catalysis Today, 295*, 110–118.

Donauerová, A., Bujdák, J., Smolinská, M., & Bujdáková, H. (2015). Photophysical and antibacterial properties of complex systems based on smectite, a cationic surfactant and methylene blue. *Journal of Photochemistry and Photobiology B: Biology, 151*, 135–141.

Dontsova, T. A., Kulikov, L. M., & Astrelin, I. M. (2017). Adsorption photocatalytic properties of micronic and graphene (2D) nanoparticles of molybdenum dichalcogenides. *Journal of Water Chemistry and Technology, 39*, 132–137.

Dontsova, T. A., Yanushevskaya, E. I., Nahirniak, S. V., Makarchuk, O. V., Ivanets, A. I., Roshchina, M. Y., Kutuzova, A. S., & Kulikov, L. M. (2018). Directional control of the structural adsorption properties of clays by magnetite modification. *Journal of Nanomaterials, 2018*, 6573016.

Fatimaha, I., Nurillahia, R., Sahronia, I., & Muraza, O. (2019). TiO_2-pillared saponite and photosensitization using a ruthenium complex for photocatalytic enhancement of the photodegradation of bromophenol blue. *Applied Clay Science, 183*, 105302.

Gregg, S. J. & Sing, K. S. W. (1982). Adsorption, Surface Area and Porosity. *Second Printing. London and New York*: *Academic Press,* 303 pp.

Hammett, L. P., & Deyrup, A. J. (1932). A series of simple basic indicators. I. The acidity functions of mixtures of sulfuric acids with water. *Journal of the American Chemical Society, 54*, 2721–2739.

Hover, V. C., Walter, L. M., Peacor, D. R., & Martini, A. M. (1999). Mg-smectite authigenesis in a marine evaporative environment, Salina Ometepec, Baja California. *Clays and Clay Minerals, 47*, 252–268.

Hu, K. H., Hu, X. G., Xu, Y. F., & Pan, X. Z. (2010). The effect of morphology and size on the photocatalytic properties of MoS_2. *Reaction Kinetics, Mechanisms and Catalysis, 100*, 153–163.

Kumaresan, S., Radheshyam, R. P., Bhavesh, D. K., & Hari, C. B. (2019). Synthesis of saponite based nanocomposites to improve the controlled oral drug release of model drug quinine hydrochloride dihydrate. *Pharmaceuticals, 12*, 105.

López-Galindo, A., Viseras, C., & Cerezo, P. (2007). Compositional, technical and safety specifications of clays to be used as pharmaceutical and cosmetic products. *Applied Clay Science, 36*, 51–63.

Makarchuk, O., Dontsova, T. & Krymets, G. (2017a). Magnetic mineral nanocomposite sorbents for removal of surfactants. *Proceedings of the 2017 IEEE 7th International Conference on Nanomaterials: Applications & Properties* (*NAP-2017*): 2017-January, 02MFPM02.

Makarchuk, O., Dontsova, T., Perekos, A., Skoblik, A., & Svystunov, Y. (2017c). Magnetic mineral nanocomposite sorbents for wastewater treatment. *Journal of Nanomaterials, 2017*, 8579598.

Makarchuk, O., Dontsova, T., & Perekos, A. (2017b). Magnetic nanocomposite sorbents on mineral base. *Springer Proceedings in Physics, 195*, 705–719.

Murray, H. H. (1999). Applied clay mineralogy today and tomorrow. *Clay Minerals, 34*, 39–49.

Mykhailenko, N., Makarchuk, O., Dontsova, T., Gorobets, S., & Astrelin, I. (2015). Purification of aqueous media by magnetically operated saponite sorbents. *Eastern-European Journal of Enterprise Technologies, 4*, 13–20.

Nityashree, N., Price, C. A. H., Pastor-Perez, L., Manohara1, G. V., Garcia, S., Maroto-Valer, M. M., & Reina, T. R. (2020). Carbon stabilised saponite supported transition metal-alloy catalysts for chemical CO_2 utilisation via reverse water-gas shift reaction. *Applied Catalysis B: Environmental, 261*, 118241.

Petra, L., Billik, P., Melichová, Z., & Komadel, P. (2017). Mechanochemically activated saponite as materials for Cu^{2+} and Ni^{2+} removal from aqueous solutions. *Applied Clay Science, 143*, 22–28.

Polyakov, V. E., & Tarasevich, Y. I. (2012). Ion exchange equilibria involving uncharged cations on saponite. *Journal of Water Chemistry and Technology, 34*, 18–27.

Puziy, A. M., Poddubnaya, O. I., Kochkin, Y. N., Vlasenko, N. V., & Tsyba, M. M. (2010). Acid properties of phosphoric acid activated carbons and their catalytic behavior in ETBE synthesis. *Carbon, 48*, 706–713.

Qiao, X. Q., Hu, F. C., Tian, F. Y., Hou, D. F., & Li, D. S. (2016). Equilibrium and kinetic studies on MB adsorption by ultrathin 2D MoS_2 nanosheets. *RSC Advances, 6*, 11631–11636.

Rodriguez, V. M. A., Suarez, B. M., Lopez, G. J. D., & Bañares, M. M. A. (1994). Acid Activation of a Ferrous Saponite (Griffithite): Physico-Chemical Characterization and Surface Area of the Products Obtained. *Clays and Clay Minerals, 42*, 724–730.

Samara, E., Matsi, T., Zdragas, A., & Barbayiannis, N. (2019). Use of clay minerals for sewage sludge stabilization and a preliminary assessment of the treated sludge's fertilization capacity. *Environmental Science and Pollution Research, 26*, 35387–35398.

Shao, H., & Pinnavaia, T. J. (2010). Synthesis and properties of nanoparticle forms saponite clay, cancrinite zeolite and phase mixtures thereof. *Microporous Mesoporous Materials, 133*, 10–17.

Sokol, H., Sprynskyy, M., Ganzyuk, A., Raks, V., & Buszewski, B. (2019). Structural, mineral and elemental composition features of iron-rich saponite clay from Tashkiv deposit (Ukraine). *Colloids Interfaces, 3*, 10.

Sprynskyya, M., Sokolb, H., Rafińskaa, K., Brzozowskaa, W., Railean-Plugarua, V., Pomastowskic, P., & Buszewskia, B. (2019). Preparation of AgNPs/saponite nanocomposites without reduction agents and study of its antibacterial activity. *Colloids and Surfaces B: Biointerfaces, 180*, 457–465.

Szabo´, T., Mitea, R., Leeman, H., Premachandra, G. S., Johnston, C. T., Szekeres, M., De'ka'ny, I., & Schoonheydt, R. A. (2008). Adsorption of protamine and papain proteins on saponiteıo. *Clays and Clay Minerals, 56*, 494–504.

Tanabe, K., Misono, M., Hattori, H., & Ono, Y. (1990). Solid Acids and Bases. *Studies in Surface Science and Catalysis, 51*, 364.

Tangaraj, V., Janot, J. M., Jaber, M., Bechelany, M., & Balme, S. (2017). Adsorption and photophysical properties of fluorescent dyes over montmorillonite and saponite modified by surfactant. *Chemosphere, Elsevier, 184*, 1355–1361.

Tarasevich, J. I., Poljakov, V. E., Ivanova, Z. G., & Trifonova, M. Y. (2011). Composition, structure and thermal stability of exchangeable cations hydrates of saponite. *Journal of Water Chemistry and Technology, 33*, 381–391.

Treiman, A. H., Morris, R. V., Agresti, D. G., Graff, T. G., Achilles, C. N., Rampe, E. B., Bristow, T. F., Ming, D. W., Blake, D. F., Vaniman, D. T., Bish, D. L., Chipera, S. J., Morrison, S. M., & Downs, R. T. (2014). Ferrian saponite from the Santa Monica Mountains (California, U.S.A., Earth): Characterization as an analog for clay minerals on Mars with application to Yellowknife Bay in Gale Crater. *American Mineralogist, 99*, 2234–2250.

Vasilyeva, I. G., Asanov, I. P., & Kulikov, L. M. (2015). Experiments and consideration about surface nonstoichiometry of few-layer MoS_2 prepared by chemical vapor deposition. *The Journal of Physical Chemistry C, 119*, 23259–23267.

Villarroel-Rocha, J., Barrera, D., & Sapag, K. (2014). Introducing a self-consistent test and the corresponding modification in the Barrett, Joyner and Halenda method for pore-size determination. *Microporous and Mesoporous Materials, 200*, 68–78.

Vlasenko, N. V., Kochkin, Y. N., Telbiz, G. M., Shvets, A. V., & Strizhak, P. E. (2019a). Insight into the active sites nature of zeolite H-BEA for liquid phase etherification of isobutylene with ethanol. *RSC Advances, 9*, 35957–35968.

Vlasenko, N. V., Kyriienko, P. I., Valihura, K. V., Yanushevska, O. I., Soloviev, S. O., & Strizhak, P. E. (2019b). Effect of Modifying Additives on the Catalytic Properties of Zirconia in the process of Ethanol Conversion to 1-Butanol. *Theoretical and Experimental Chemistry, 55*, 40–46.

Vogels, R. J. M. J., Kloprogge, J. T., & Geus, J. W. (2005). Synthesis and characterization of saponite clays. *American Mineralogist, 90*, 931–944.

Zhoua, C. H., Zhoua, Q., Wua, Q. Q., Petitd, S., Jianga, X. C., Xiaa, S. T., Lib, C. S., & Yua, W. H. (2019). Modification, hybridization and applications of saponite: An overview. *Applied Clay Science, 168*, 136–154.

(*Received 16 October 2019; revised 24 Jun 2020; AE: Peter Ryan***)**

https://doi.org/10.1007/s42860-020-00088-4 Published online by Cambridge University Press